Bioconjugate Chemistry

Article

pubs.acs.org/bc

# Development of a New Dumbbell-Shaped Decoy DNA Using a Combination of the Unnatural Base Pair $ImO^N$:$NaN^O$ and a CuAAC Reaction

Yosuke Higuchi, Kazuhiro Furukawa, Tadashi Miyazawa, and Noriaki Minakawa*

Graduate School of Pharmaceutical Sciences, The University of Tokushima, Shomachi 1-78-1, Tokushima 770-8505, Japan

Supporting Information

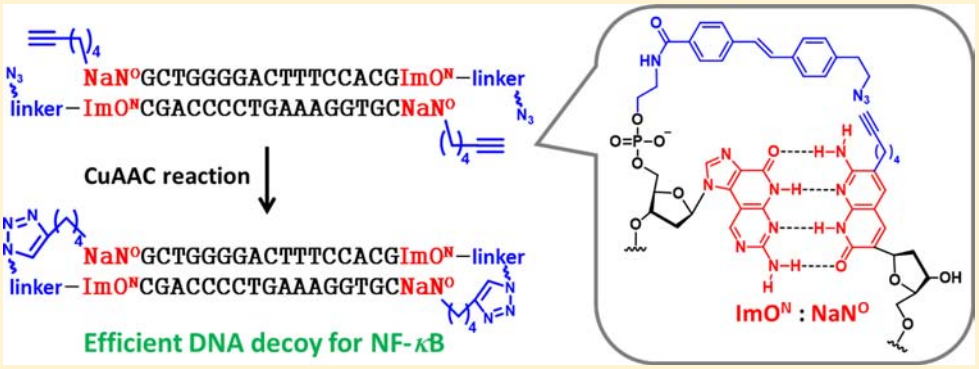


**ABSTRACT:** We describe the synthesis and potential application of a new dumbbell-shaped decoy DNA prepared using a combination of the base pair $ImO^N$:$NaN^O$ and a copper-catalyzed azide–alkyne cycloaddition (CuAAC) reaction. The CuAAC reaction between the azido group on the 5′-end of oligodeoxynucleotide (ODN) and the ethynyl group on the $NaN^O$ base of the opposite strand did not proceed, whereas that between the azido group and the flexible hexynyl group on the $NaN^O$ base of the opposite strand proceeded smoothly to give a new dumbbell-shaped double-stranded ODN (dsODN). The resulting dsODN had extremely high thermal stability and exhibited exonuclease resistance. In addition, the terminal modification did not affect its helical structure, and thus, the dumbbell-shaped dsODN displayed promising in vitro activity in a competition assay with the NF-*k*B p50 transcription factor homodimer.

## INTRODUCTION

The expression of numerous genes is regulated by transcription factors,[1] which are proteins that bind to specific DNA sequences in genomic promoters and determine whether the DNA sequence is transcribed into mRNAs. Transcriptional misregulation induces various diseases, such as inflammatory stress response, cardiovascular defect, and cancer.[2] Recent studies have revealed that the expression of noncording RNAs, such as microRNA, is also regulated by the corresponding transcription factors.[3,4] Thus, regulation of the transcription factors is crucial for treating diseases and for clarifying complicated gene networks.

Decoy DNA can be used to regulate transcription factors in eukaryotic systems.[5] In general, decoy DNAs are composed of short double-stranded oligodeoxynucleotides (dsODNs) containing the binding sequence of the transcription factor, which prevents the transcription factor from binding to the genomic promoter. Thus, the binding of the transcription factor to the decoy DNAs inhibits transcription. A large number of decoy DNAs have been developed for various transcription factors to inhibit gene expression with high specificity.[6−9] However, decoy DNAs have several issues. For instance, short dsODNs have relatively low thermal stability under physiological conditions. Moreover, they are easily degraded by nucleases in biological fluids.

To improve the thermal stability and nuclease resistance of decoy DNAs, various chemical modifications have been reported. One promising approach to overcome the aforementioned drawbacks is to use dumbbell-shaped dsODNs, which exhibit high thermal stability and exonuclease resistance since the dsODNs have no terminal nucleotide residues.[10,11] Because of the difficulty in preparing large quantities of dumbbell-shaped DNAs by using enzymatic reactions, researchers have attempted chemical cross-linking reactions at the termini of the dsODNs.[12−14] Copper-catalyzed azide–alkyne cycloaddition (CuAAC)[15,16] is a promising method for preparing cross-linked dsODN. Nakane et al. have prepared thymidine derivatives containing azide and alkyne groups for cross-linking dsODNs at their 3′ and 5′ termini, respectively.[12] The CuAAC reaction on dsODNs rapidly proceeds to afford cross-linked dumbbell-shaped dsODN. However, the resulting triazole-linked DNA containing a T–T mismatch loop-out

**Received:** May 20, 2014
**Revised:** June 10, 2014
**Published:** June 26, 2014

   dx.doi.org/10.1021/bc500225r | *Bioconjugate Chem.* 2014, 25, 1360−1369

structure causes a decrease in the endonuclease resistance. Therefore, a more effective and versatile method for preparing decoy DNAs is required for this strategy to be useful.

Our group has previously reported the utility of an unnatural imidazopyridopyrimidine:naphthyridine (Im:Na) base pair containing four hydrogen bonds for preparing thermally stabilized decoy DNAs.[17,18] The resulting short dsODNs containing $ImO^N$:$NaN^O$ pairs at their termini are thermally stabilized without affecting their helical structure. In addition, these decoy DNAs, which act as strong competitors to the natural NF-κB binding duplex, are resistant to nuclease digestion in spite of possessing a natural phosphodiester linkage. On the bases of the above results, we developed a method for preparing new dumbbell-shaped decoy DNA using a combination of the $ImO^N$:$NaN^O$ pair and a CuAAC reaction (Figure 1) and prepared the desired decoy DNA without any loop-out structure, which can cause a decrease in the nuclease resistance. This decoy DNA showed potent binding affinity against NF-κB because of its high thermal stability and nuclease resistance. This paper describes the synthesis, properties, and application of decoy DNA containing the $ImO^N$:$NaN^O$ pair.

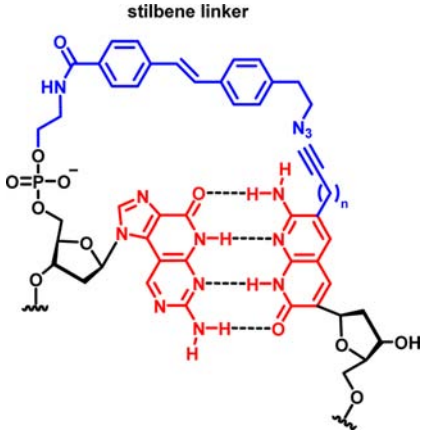


**Figure 1.** Terminal structure to prepare the new dumbbell-shaped decoy DNA.

## RESULTS AND DISCUSSION

**Synthesis of Alkynyl-$NaN^O$ Nucleosides and Stilbene Linker.** The synthetic strategy for preparing the newly designed decoy molecule is shown in Figure 1. The alkynyl group was attached to the 6-position of the $NaN^O$ base at the 3′-end of the ODN. To investigate the effects of the flexibility of the alkynyl group on the CuAAC reaction, $NaN^O$ derivatives having either an ethynyl group or a hexynyl group were prepared. The azide group was attached to the 5′-end of the complementary ODN via a stilbene linker. It is known that stilbene derivatives stack on the terminal base pairs at the 5′-end.[19] Thus, it is anticipated that the azide group coupled with the stilbene linker can approach the alkynyl group on the $NaN^O$ base at the 3′-end of the opposite strand, increasing the efficiency of the click reaction. To construct the terminal structure, we synthesized alkynyl-$NaN^O$ nucleosides attached to controlled pore glass (CPG) and the stilbene linker. In addition, the phosphoramidite unit of $ImO^N$ was synthesized according to our previous method.[20]

The synthesis of alkynyl-$NaN^O$ nucleosides attached to CPG is shown in Scheme 1. Starting with $NaN^O$,[17] this was treated with *tert*-butyldimethylsilyl chloride (TBSCl) to give silylated-$NaN^O$ **1**. Then treatment of **1** with *N*-iodosuccinimide (NIS) in DMF gave 6-iodo derivative **2**. This iodination must be carried out prior to the protection of 7-amino group because of the steric bulk of the protecting group (i.e., dibutylaminomethylidene group). The resulting **2** was transformed into **3** by using a Sonogashira coupling reaction with trimethylsilylacetylene (TMS acetylene). After removing the TBS and TMS groups to afford **4**, it was treated with *N*,*N*-dibutylformamide dimethylacetal (DBF dimethylacetal) to give **5**. Then, **5** was converted into **7** via **6** by dimethoxytritylation of the 5′-hydroxyl group, followed by succinylation of the 3′-hydroxyl group. Finally, CPG-linked ethynyl-$NaN^O$ nucleoside **8** was prepared by linking **7** to the resin. Hexynyl-$NaN^O$ nucleoside **13** was prepared as follows. Treatment of the 6-iodo derivative **2** with 4-pentyn-1-ol afforded **9**. The resulting **9** was converted into aldehyde **11** via catalytic hydrogenation, followed by oxidization of the primary hydroxyl group. Then, **11** was treated with the Ohira-Bestmann reagent to give **12**. CPG-linked hexynyl-$NaN^O$ nucleoside **17** was prepared using the same method as that described for **8**.

The synthesis of the stilbene linker is shown in Scheme 2. Starting with **18**,[21] its bromo group was converted into the acetoxy group. Heck coupling reaction of the resulting **19** with 4-iodobenzoic acid gave stilbene derivative **20**. Then, **20** was condensed with silylated ethanolamine to give **21**. To convert the acetoxy group into the desired bromo group, **21** was treated with NaOMe, followed by methanesulfonyl chloride (MsCl) and lithium bromide (LiBr) to give **22**. Finally, **22** was converted into the corresponding phosphoramidite unit **23**. In order to conduct the CuAAC reaction, the stilbene linker must have an azide group instead of a bromo group. However, since the azide group is known to be readily reduced by trivalent phosphorus atoms,[22] it was converted into the azide group after solid-phase ODN synthesis (see the Experimental Procedures).

**Synthesis of Precursor ODNs and Their Cross-Linking by Using a CuAAC Reaction.** To examine the cross-linking between the azide and the ethynyl groups by using a CuAAC reaction, **ODN 1** ($n$ = 0) and **ODN 2** ($n$ = 4), and their complementary **ODN 3** ($n$ = 0) and **ODN 4** ($n$ = 4) were prepared using the $ImO^N$ phosphoramidite unit,[20] stilbene phosphoramidite unit **23**, and CPG resin supporting alkynyl-$NaN^O$ nucleoside **8** or **17**, followed by azidation on the CPG (Figure 2a). A CuAAC reaction between **ODN 1** and **ODN 3** in 0.1 M MOPS buffer (pH 7.0) and 1 M NaCl containing 10 equiv of $CuSO_4$ and 2 mM sodium ascorbate at room temperature was tried, and the progress of the reaction was monitored by using reversed-phase HPLC. In this case, the desired product was not detected, and degradation of the starting ODNs was observed with an increase in the reaction time (data not shown). On the other hand, the reaction between **ODN 2** and **ODN 4** under the same conditions proceeded smoothly probably due to the flexibility of the alkynyl tether. As shown in Figure 2b, two new peaks were observed after 10 min. The slower peak gradually decreased as well as that for the starting dsODN, whereas the one left to the starting material (with a faster retention time) increased and was the only peak present after 3 h. From these HPLC profiles, it was assumed that the intermediate peak corresponded to a hairpin-like product, which was cross-linked on one side, and the faster peak (retention time = 14.5 min) was the desired dumbbell-shaped product, **decoy 1**, which was cross-linked on both sides. Although a peak in the MALDI-TOF mass spectrum


dx.doi.org/10.1021/bc500225r | *Bioconjugate Chem.* 2014, 25, 1360−1369

**Scheme 1**[a]

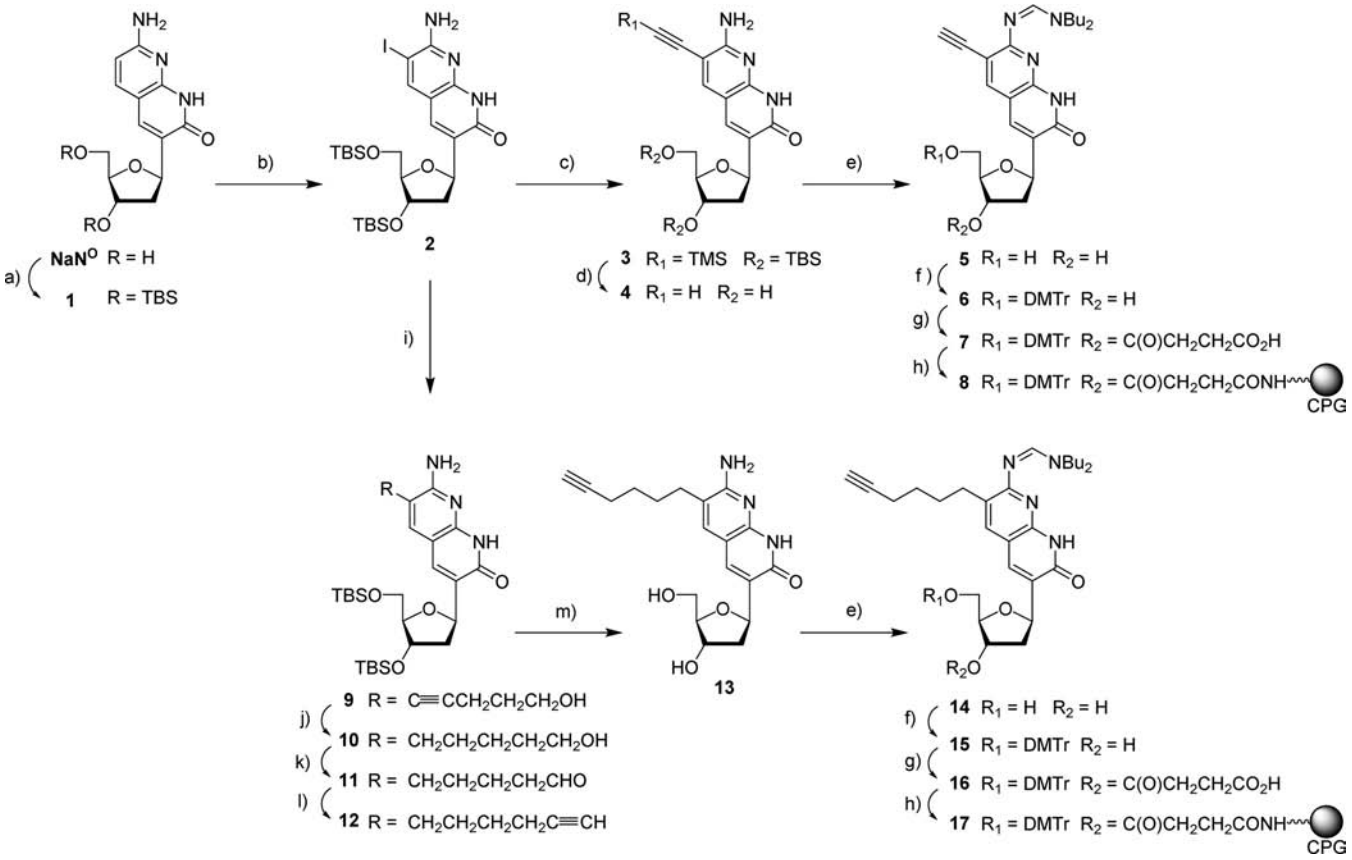


[a]Reagents and conditions: (a) TBSCl, imidazole, DMF, 88%; (b) NIS, DMF, 81%; (c) TMS acethylene, CuI, $PdCl_2(PPh_3)_2$, $Et_3N$, DMF, 97%; (d) TBAF, THF, 98%; (e) DBF dimethylacetal, DMF, 59% (44% for **14**); (f) DMTrCl, pyridine, 91% (74% for **15**); (g) succinic anhydride, $Et_3N$, DMAP, MeCN, 78% (70% for **16**); (h) CPG-resin, HBTU, HOBt, DIEA, MeCN, then $Ac_2O$, DMAP, pyridine; (i) 4-pentyn-1-ol, $PdCl_2(PPh_3)_2$, CuI, $Et_3N$, MeCN, quant; (j) Pd/C, ammonium formate, MeOH, 98%; (k) $SO_3$-py, $Et_3M$, DMSO, $CH_2Cl_2$, 63%; (l) Ohira-Bestmann reagent, $K_2CO_3$, MeOH, $Et_2O$; (m) TBAF, THF, 2 steps 88%.

**Scheme 2**[a]

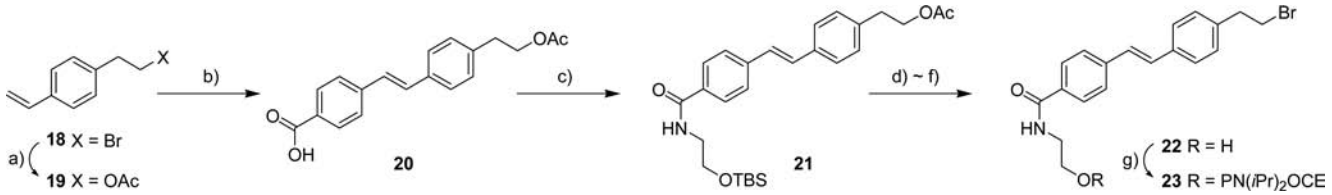


[a]Reagents and conditions: (a) NaOAc, DMF, 64%; (b) 4-iodobenzoicacid, $Pd(OAc)_2$, $Et_3N$, DMF, 83%; (c) $NH_2CH_2CH_2OTBS$, HBTU, HOBt, DIEA, DMF, 73%; (d) NaOMe, MeOH; (e) MsCl, $Et_3N$, $CH_2Cl_2$; (f) LiBr, acetone, then $H_2O$, 3 steps 88%; (g) $CEOPN(iPr)_2Cl$, DIEA, MeCN, 62%.

for the product corresponding to the faster peak was observed at $m/z$ = 12 779.6 (calculated mass: 12 772.4), which corresponds to the desired structure, the hairpin-like product has the same molecular weight. Therefore, complete enzymatic digestion by snake venom phosphodiesterase (SVPD), nuclease P1, and calf intestine alkaline phosphatase of the product corresponding to the faster peak was performed to confirm the structure (Figure 3). If it is the correct structure, the $ImO^N$, a triazole-bridged $NaN^O$ nucleoside with stilbene linker (see compound **S4** in the Supporting Information), and the natural nucleosides (dA, dC, dG, and dT) should be observed in the HPLC profile. The HPLC profiles were obtained at 260 and 330 nm to detect the natural nucleosides and the unnatural nucleosides, such as $ImO^N$ and $NaN^O$ derivative **S4**, respectively. For comparison, **ODN 1** was also subjected to complete digestion. The HPLC profiles of the **ODN 1** digestion showed peaks corresponding to the natural nucleosides at 260 nm, and $ImO^N$, hexynyl-$NaN^O$ **13**, and the azide-modified stilbene linker at 330 nm, respectively. On the other hand, the HPLC profiles for the faster peak digestion showed no peaks corresponding to hexynyl-$NaN^O$ **13** and the azide-modified stilbene linker, although they showed a new peak at 34 min along with the peak for $ImO^N$. This new peak was identical to that for a separately prepared authentic sample of **S4** (see Scheme S1 in the Supporting Information). Thus, it was confirmed that the desired CuAAC reaction occurred at


dx.doi.org/10.1021/bc500225r | *Bioconjugate Chem.* 2014, 25, 1360−1369

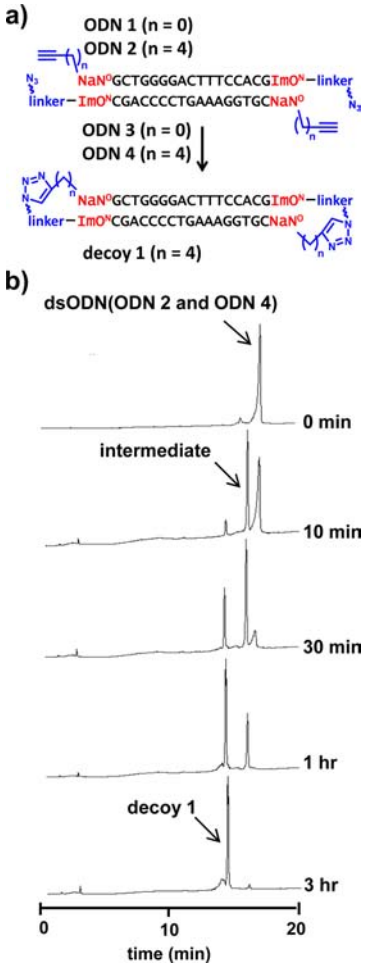


**Figure 2.** CuAAC reaction between **ODN 2** and **ODN 4** to prepare **decoy 1**. (a) Sequences and structures of **ODN 1**–**ODN 4** and **decoy 1**. (b) HPLC profiles of the reaction between **ODN 2** and **ODN 4**. The reaction was carried out with 10 mM of each ODN in a 100 mM MOPS–NaOH (pH 7.0) buffer containing 1 M NaCl, 100 mM $CuSO_4$–TBTA complex, and 2 mM sodium ascorbate.

both termini of the dsODN and that the desired dumbbell-shaped DNA was synthesized.

**Properties and Structural Aspects of the Dumbbell-Shaped DNA.** Prior to evaluation of the potency of **decoy 1**, its properties and structural aspects were examined. In addition to **decoy 1**, we prepared three control decoys (**decoy 2**, **decoy 3**, and **decoy 4**) to evaluate the efficiency of the hybrid modification. As shown in Figure 4, **decoy 2**, which is not cross-linked but contains the ImO$^N$:NaN$^O$ pair and stilbene linker for stabilization, is a precursor for **decoy 1**, and **decoy 3** has only ImO$^N$:NaN$^O$ pairs at both termini. In addition, natural **decoy 4** was prepared.

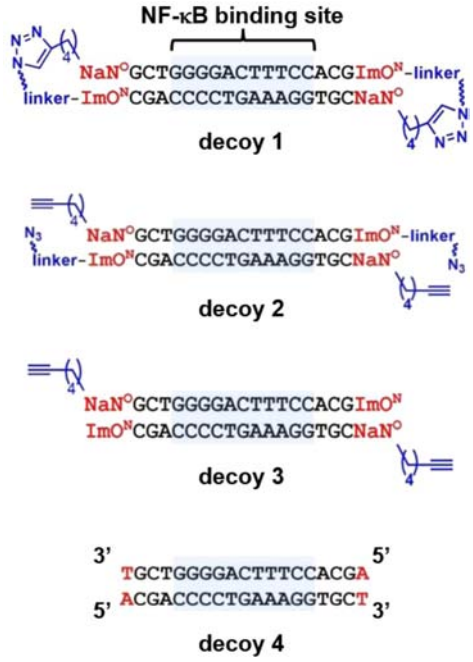


**Figure 4.** Sequences and the terminal structures of the decoys.

We first analyzed the thermal stability of each decoy by using UV melting experiments (Table 1). The melting temperature ($T_m$) for **decoy 3** was 59.6 °C, which was 5.3 °C higher than that of **decoy 4**. This is consistent with our previous report, in which the ImO$^N$:NaN$^O$ pairs at both termini stabilize the duplex by +5.1 °C.[18] The $T_m$ value for **decoy 2** was 67.8 °C,

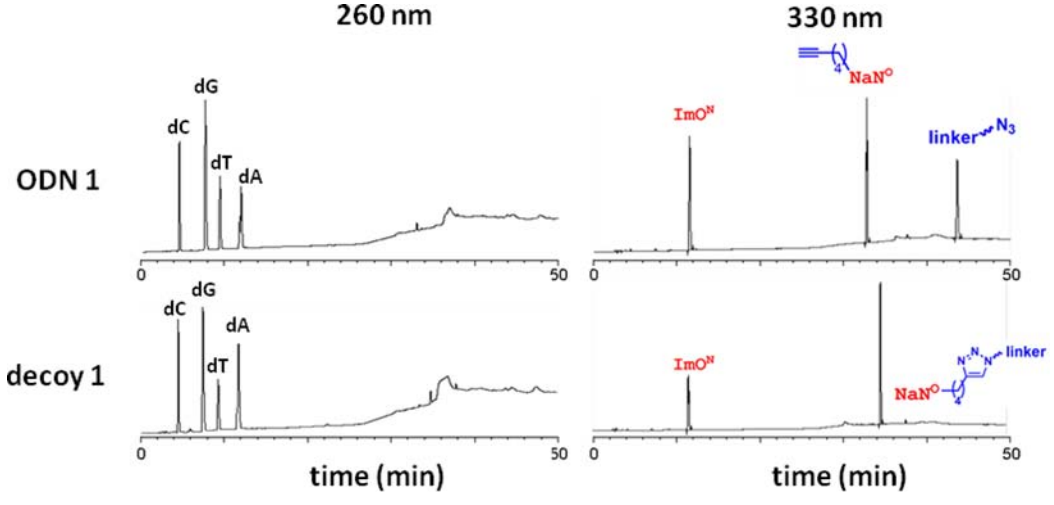


**Figure 3.** HPLC profiles of enzymatic digestion of **ODN 1** and **decoy 1**. The products were detected at 260 and 330 nm, respectively.


dx.doi.org/10.1021/bc500225r | *Bioconjugate Chem.* 2014, 25, 1360–1369

Table 1. Hybridization Data of the Decoy Molecules[a]

| | $T_m$ (°C) | $\Delta T_m$[b] (°C) |
|---|---|---|
| **decoy 1** | >90 | >35.7 |
| **decoy 2** | 67.8 | 13.5 |
| **decoy 3** | 59.6 | 5.3 |
| **decoy 4** | 54.3 | - |

[a]The values were obtained in a 1 mM Na cacodylate buffer containing 1.2 $\mu$M dsDNA and 1 mM NaCl, and are the average of three independent analyses. [b]$\Delta T_m = T_m$ (each decoy) − $T_m$ (**decoy 4**).

which was 13.5 °C higher than that of **decoy 4** and 8.2 °C higher than that of **decoy 3**. This result indicates that the stacking effect of the stilbene linker on the terminal $ImO^N$:$NaN^O$ pairs contributes to the stabilization of the duplex.[19] As expected, the $T_m$ value for cross-linked **decoy 1** was higher than 90 °C, which was significantly higher (>35.7 °C) than that for **decoy 4**. Therefore, modifying the decoy with $ImO^N$:$NaN^O$ pairs, a stilbene linker, and triazole-cross-linking resulted in a drastic increase in thermal stability of the duplex.

We next investigated the enzymatic stability of each decoy against 3′-exonucleases, which are dominant in human serum. First, we examined the stability against SVPD, which degrades ODN from its 3′-end. After incubating each decoy in an appropriate buffer containing SVPD, the reaction was analyzed by using denaturing polyacrylamide gel electrophoresis and ethidium bromide staining. The half-lives ($t_{1/2}$s) were determined from the residual ratio of the starting material (full length ODN) at each time. However, all decoys except for natural **decoy 4** were stable probably due to the $ImO^N$:$NaN^O$ pairs at the termini (data not shown). Next, we investigated the stability against exonuclease III, which also degrades dsODN from its 3′-end. As shown in Figure 5 (also see Figure S1 in the


**Figure 5.** Stability of each decoy against Exonuclease III. Each decoy (10 $\mu$M) was incubated with Exonuclease III (10 U) in 50 mM Tris-HCl (pH 8.0), 5 mM $MgCl_2$, and 1 mM DTT (total volume 20 $\mu$L) at 37 °C and then subjected to 16% denatured PAGE.

Supporting Information), **decoy 4** rapidly degraded, and its $t_{1/2}$ value was determined to be 0.8 min. On the other hand, **decoy 2** and **decoy 3** showed relatively higher resistance to exonuclease III than **decoy 4** did, and their $t_{1/2}$ values were calculated to be 4.7 and 3.8 min, respectively. This suggested that the introduction of $ImO^N$:$NaN^O$ pairs increased the resistance against exonuclease III, as previously reported.[18] As expected, the $t_{1/2}$ value for **decoy 1** was >30 min; that is, it shows a robust resistance to exonuclease III. Thus, modification of the terminal structure and cross-linking increase the stability of decoy DNA.

Previously, we have reported that introduction of unnatural $ImO^N$:$NaN^O$ pairs on the termini of dsODN does not affect its helical structure.[18] This is an important matter to apply it as the decoy molecule. The substrate prepared in this work was cross-linked via the stilbene linker. To investigate the effect of these modifications on the helical structure, circular dichroism (CD) spectra of **decoy 1** as well as **decoy 2**−**decoy 4** were acquired. Natural **decoy 4** showed a typical B-form spectrum with a positive Cotton effect around 280 nm and a negative Cotton effect around 240 nm, and the modified decoys (**decoy 1**−**decoy 3**) showed similar spectrum to that of **decoy 4**, indicating that our modifications of the termini had little effect on the helical structure (Figure S2 in the Supporting Information). In other words, the new dumbbell-shaped decoy DNA showed high thermal stability and excellent resistance against 3′-exonuclease while maintaining its helical structure.

**Competitive Binding Assay of Decoy DNAs to NF-κB.** We evaluated the ability of **decoy 1** to act as a decoy molecule against NF-κB, which is a transcriptional factor and is important in many signal transduction pathways in the immune system, using a competitive binding assay. The assay was carried out in an appropriate buffer solution containing NF-κB p50 homodimer (25 ng/$\mu$L) and $^{32}$P-radiolabeled **decoy 4** (10 nM) at various concentrations of the nonlabeled decoys. The dissociation of the complex of 5′-$^{32}$P-labeled **decoy 4** and NF-κB was analyzed by using an electrophoretic mobility shift assay (Figure 6a), and the ratio of the complex was plotted against the concentration of the decoy to afford $IC_{50}$ values (Figure 6b). An increase in the nonlabeled competitor decoy decreased the ratio of the complex, and the $IC_{50}$ values were estimated to be 56.4 (**decoy 1**), 94.9 (**decoy 2**), 92.2 (**decoy 3**), and 123.2 nM (**decoy 4**). Among the three modified decoys, **decoy 1** showed the highest binding affinity, and **decoy 2** and **decoy 3** showed better affinity than natural **decoy 4**. This trend is consistent with the thermal stabilities (Table 1), indicating that thermal stability is a crucial factor when designing efficient decoy molecules.

Nakane et al. have reported that the insertion of consecutive thymidine residues at the terminal of dumbbell-shaped decoys, which can potentially generate a loop-out structure, increases the affinity to NF-κB since terminal cross-linking without a loop structure causes structural changes in dsODNs. Contrary to their work, our results showed that no loop-out structure was needed to exhibit potent affinity to NF-κB. As described above, we have developed a new dumbbell-shaped decoy DNA with high thermal stability and strong resistance without any changes in its helical structure by using the unnatural base pair $ImO^N$:$NaN^O$ and a CuAAC reaction.

## ■ CONCLUSION

In this study, we prepared a new dumbbell-shaped decoy DNA. Using the unnatural base pair $ImO^N$:$NaN^O$ and a CuAAC reaction afforded the desired dsODN effectively without causing changes in its helical structure. In addition, the resulting decoy DNA showed high thermal stability and exonuclease resistance due to synergistic effects of the hybrid modifications, and we showed that it acts as a potent NF-κB decoy molecule. It is worth noting that the dumbbell-shaped DNA prepared by using our method does not include any single strand regions, such as hairpin and loop-out structures. Therefore, this new dumbbell-shaped decoy DNA should be resistant against not only exonucleases but also endonucleases. Since it should be possible to prepare dumbbell-shaped RNAs[23]

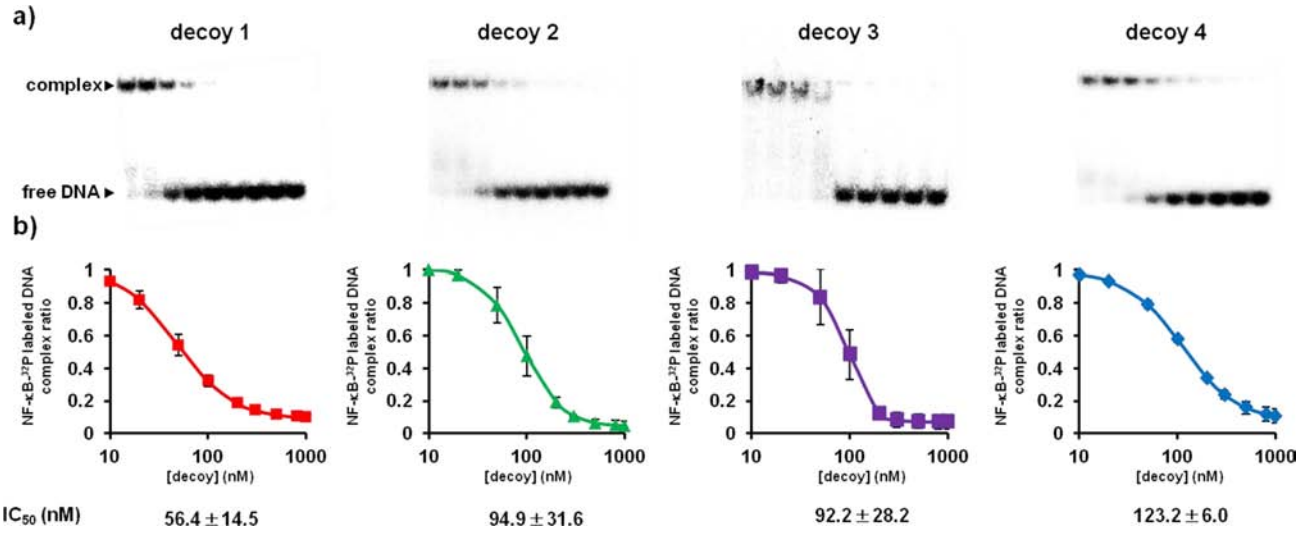


**Figure 6.** Effects of the decoys on the interaction with the NF-κB p50 homodimer and electromobility shift assays with NF-κB. (a) Native PAGE analysis. Competition experiments were performed by incubating NF-κB p50 homodimer (25 ng/μL) and $^{32}$P-radiolabeled **decoy 4** (10 nM) with different concentrations of each decoy. (b) Plots of the complex ratio against the concentration of each decoy, which were used to obtain $IC_{50}$ values. Each $IC_{50}$ value was calculated by using three independent experiments.

as well as dumbbell-shaped DNAs using this method, we are currently investigating a variety of applications.

## EXPERIMENTAL PROCEDURES

Physical data were measured as follows: Melting points are uncorrected. $^1$H and $^{13}$C NMR spectra were recorded at 400 or 500 MHz and 100 or 125 MHz instruments (Bruker FT-NMR AV400 or AV500) in $CDCl_3$ with tetramethylsilane as an internal standard or DMSO-$d_6$ as the solvent. Chemical shifts are reported in parts per million ($\delta$), and signals are expressed as s (singlet), d (doublet), t (triplet), q (quartet), m (multiplet), or br (broad). All exchangeable protons were detected by addition of $D_2O$. TLC was done on Merck Kieselgel F254 precoated plates. Silica gel used for column chromatography was KANTO CHEMICAL Silica Gel 60 (spherical) 63-210 mesh or Silica Gel 60 N (spherical, neutral) 63-210 mesh. Mass spectrum analysis was carried out with LCT Premier (Waters). CD spectrum was analyzed by J-1500 (JASCO).

**7-Amino-3-[2-deoxy-3,5-bis-*O*-(*tert*-butyldimethylsilyl)-β-D-ribofuranosyl]-1*H*-1,8-naphthyridin-2-one (1).** To a solution of NaN$^O$ (693 mg, 2.5 mmol) in DMF (10 mL) were added imidazole (816 mg, 12 mmol) and TBSCl (904 mg, 6.0 mmol), and the mixture was stirred at room temperature for 12 h. The reaction was quenched by addition of ice, and the solvent was evaporated. The residue was partitioned between AcOEt and $H_2O$, and the organic layer was washed with $H_2O$, saturated aqueous $NaHCO_3$, and brine. The organic layer was dried ($Na_2SO_4$), and evaporated. The residue was purified by a silica gel column, eluted with 0−2% MeOH in $CHCl_3$, to give **1** (1.11 g, 88%, as a pale yellow solid): ESI-LRMS $m/z$ 506 ($MH^+$); ESI-HRMS calcd for $C_{25}H_{43}N_3O_4NaSi_2$ 528.2690, found 528.2748. $^1$H NMR ($CDCl_3$): $\delta$ 13.30 (brs, 1 H), 7.78 (s, 1 H), 7.53 (d, 1 H, $J$ = 8.5 Hz), 6.85 (br s, 2 H), 6.31 (d, 1 H, $J$ = 8.5 Hz), 5.29 (dd, 1 H, $J$ = 6.5 and 8.5 Hz), 4.35 (dt, 1 H, $J$ = 3.0 and 5.8 Hz), 3.93 (m, 1 H), 3.77 (dd, 1 H, $J$ = 3.8 and 10.8 Hz), 3.70 (dd, 1 H, $J$ = 5.0 and 10.8 Hz), 2.43 (ddd, 1 H, $J$ = 2.8, 6.2, and 12.6 Hz), 1.85 (m, 1 H), 0.91 (m, 18 H), 0.10 (m, 12 H); $^{13}$C NMR ($CDCl_3$): $\delta$ 164.50, 160.84, 149.92, 138.19, 134.65, 129.53, 106.72, 106.68, 87.63, 75.33, 74.03, 63.89, 42.23, 26.39, 26.29, 18.80, −4.10, −4.33, −4.87, −4.93.

**7-Amino-6-iodo-3-[2-deoxy-3,5-bis-*O*-(*tert*-butyldimethylsilyl)-β-D-ribofuranosyl]-1*H*-1,8-naphthyridin-2-one (2).** To a solution of **1** (1.1 g, 2.2 mmol) in DMF (20 mL) was added NIS (643 mg, 2.8 mmol), and the whole was stirred at room temperature for 8 h. The solution was partitioned between $CHCl_3$ and 5% aqueous $Na_2S_2O_3$, and the organic layer was washed with brine. The organic layer was dried ($Na_2SO_4$) and evaporated. The residue was purified by a silica gel column, eluted with hexane/AcOEt (10:1−8:1), to give **2** (1.13 g, 81%, as a yellow solid): ESI-LRMS $m/z$ 632 ($MH^+$); ESI-HRMS calcd for $C_{25}H_{42}IN_3O_4NaSi_2$ 654.1656, found 654.1698. $^1$H NMR ($CDCl_3$): $\delta$ 12.94 (brs, 1 H), 8.00 (s, 1 H), 7.72 (s, 1 H), 5.25 (dd, 1 H, $J$ = 6.2 and 8.6 Hz), 4.35 (dt, 1 H, $J$ = 2.8 and 5.6 Hz), 3.95 (m, 1 H), 3.76 (dd, 1 H, $J$ = 3.8 and 10.8 Hz), 3.67 (dd, 1 H, $J$ = 5.3 and 10.8 Hz), 2.43 (ddd, 1 H $J$ = 2.8, 6.2, and 12.8 Hz), 1.80 (m, 1 H), 0.91 (m, 18 H), 0.05 (m, 12 H). $^{13}$C NMR ($CDCl_3$): $\delta$ 164.89, 159.01, 149.39, 137.08, 134.26, 129.44, 106.95, 94.40, 87.61, 75.12, 74.00, 64.89, 42.57, 26.29, 26.13, 18.94, 18.32, −4.09, −4.25, −4.76, −4.80.

**7-Amino-6-(5-hydroxy-pent-1-ynyl)-3-[2-deoxy-3,5-bis-*O*-(*tert*-butyldimethylsilyl)-β-D-ribofuranosyl]-1*H*-1,8-naphthyridin-2-one (9).** To a suspension of **2** (470 mg, 0.75 mmol) in MeCN (7.5 mL) and $Et_3N$ (7.5 mL) were added 4-pentyn-1-ol (0.1 mL, 1.1 mmol), $PdCl_2(PPh_3)_2$ (26 mg, 0.037 mmol) and CuI (3 mg, 0.015 mmol), and the mixture was stirred at room temperature for 20 min. The solvent was evaporated, and the residue was purified by a silica gel column, eluted with 0−4% MeOH in $CHCl_3$, to give **9** (440 mg, quant, as a pale yellow solid): ESI-LRMS $m/z$ 588 ($MH^+$); ESI-HRMS calcd for $C_{30}H_{49}N_3O_5NaSi_2$ 610.3108, found 610.3021. $^1$H NMR ($CDCl_3$): $\delta$ 13.2 (brs, 1 H), 7.69 and 7.57 (each s, each 1 H), 5.26 (dd, 1 H, $J$ = 6.6 and 8.8 Hz), 4.35 (m, 1 H), 3.95 (m, 1 H), 3.84 (t, 2 H, $J$ = 5.8 Hz), 3.76 (dd, 1 H, $J$ = 4.1 and 10.8 Hz), 3.68 (dd, 1 H, $J$ = 5.1 and 10.8 Hz), 2.62 (t, 2H, $J$ = 7.0 Hz), 2.43 (ddd, 1 H, $J$ = 3.0, 6.3, and 12.8 Hz), 1.90 (m, 2 H), 1.80 (m, 1 H), 0.91 (m, 18 H), 0.09 (m, 12 H). $^{13}$C NMR


dx.doi.org/10.1021/bc500225r | Bioconjugate Chem. 2014, 25, 1360−1369

($CDCl_3$): δ 164.07, 160.79, 148.62, 139.31, 133.75, 129.64, 106.19, 101.51, 95.78, 87.44, 75.72, 75.15, 73.91, 63.71, 61.79, 41.92, 31.45, 18.54, 18.25, 16.50, −4.35, −4.59, −5.10, −5.19.

**7-Amino-6-(5-hydroxypentyl)-3-[2-deoxy-3,5-bis-*O*-(*tert*-butyldimethylsilyl)-β-D-ribofuranosyl]-1*H*-1,8-naphthyridin-2-one (10).** To a suspension of **9** (440 mg, 0.75 mmol) in MeOH (7 mL) were added 10% Pd/C (80 mg) and ammonium formate (472 mg, 7.5 mmol), and the mixture was heated for 1.5 h under reflux. The solvent was evaporated, and the residue was suspended to $CHCl_3$. The solids were filtered through a Celite pad, and washed with $CHCl_3$. The combined filtrate and washings were evaporated to give **10** (433 mg, 98%, as a pale yellow solid): ESI-LRMS *m*/*z* 592 ($MH^+$); ESI-HRMS calcd for $C_{30}H_{53}N_3O_5NaSi_2$ 614.3421, found 614.3488. $^1H$ NMR ($CDCl_3$): δ 13.3 (brs, 1 H), 7.78 and 7.36 (each s, each 1 H), 7.06 (brs, 2 H), 5.32 (dd, 1 H, *J* = 6.8 and 8.6 Hz), 4.35 (m, 1 H), 3.95 (m, 1 H), 3.80 (dd, 1 H, *J* = 3.8 and 10.8 Hz), 3.71 (dd, 1 H, *J* = 5.0 and 10.8 Hz), 3.66 (t, 2 H, *J* = 6.4 Hz), 2.49 (m, 3 H), 1.84 (ddd, 1 H, *J* = 6.0, 9.0, and 13.0 Hz), 1.65 (m, 6 H), 0.91 (m, 18 H), 0.09 (m, 12 H). $^{13}C$ NMR ($CDCl_3$): δ 164.17, 159.23, 148.15, 135.98, 134.29, 129.06, 117.66, 106.79, 87.33, 75.14, 73.81, 63.70, 62.95, 41.97, 32.62, 30.69, 27.67, 26.16, 26.04, 18.57, 18.23, 0.14, −4.34, −4.59, −5.13, −5.17.

**7-Amino-6-pentanal-3-[2-deoxy-3,5-bis-*O*-(*tert*-butyldimethylsilyl)-β-D-ribofuranosyl]-1*H*-1,8-naphthyridin-2-one (11).** To a solution of **10** (430 mg, 0.73 mmol) in $CH_2Cl_2$ (7 mL) were added $Et_3N$ (0.4 mL, 2.9 mmol), DMSO (80 μL, 1.1 mmol), and pyridine−sulfur trioxide complex (232 mg, 1.45 mmol) at 0 °C, and the mixture was stirred at room temperature for 3 h. The mixture was partitioned between $CHCl_3$ and $H_2O$, and the extract was washed with brine. The organic layer was dried ($Na_2SO_4$) and evaporated. The residue was purified by a silica gel column, eluted with 0−2% MeOH in $CHCl_3$, to give **11** (272 mg, 63%, as a pale yellow solid): ESI-LRMS *m*/*z* 590 ($MH^+$); ESI-HRMS calcd for $C_{30}H_{52}N_3O_5Si_2$ 590.3446, found 590.3407. $^1H$ NMR ($CDCl_3$): δ 13.2 (brs, 1 H), 9.79 (s, 1H), 7.79 and 7.38 (each s, each 1 H), 7.06 (brs, 2 H), 5.30 (dd, 1 H *J* = 6.8 and 8.6 Hz), 4.36 (m, 1 H), 3.95 (m, 1 H), 3.79 (dd, 1 H, *J* = 3.8 and 10.8 Hz), 3.71 (dd, 1 H, *J* = 5.0 and 10.8 Hz), 2.49 (m, 5 H), 1.82 (m, 1 H), 1.74 (m, 4 H), 0.91 (m, 18 H), 0.10 (m, 12 H). $^{13}C$ NMR ($CDCl_3$): δ 201.80, 163.89, 158.86, 147.91, 135.80, 134.01, 128.92, 116.83, 106.55, 87.10, 74.86, 73.61, 63.46, 46.33, 43.52, 40.88, 25.89, 25.77, 21.65, 18.30, 17.97, 8.54, −4.61, −4.85, −5.39, −5.43.

**7-Amino-6-hex-5-ynyl-3-(2-deoxy-β-D-ribofuranosyl)-1*H*-1,8-naphthyridin-2-one (13).** To a suspension of **11** (270 mg, 0.46 mmol) in MeOH (10 mL) and $Et_2O$ (5 mL) were added $K_2CO_3$ (127 mg, 0.92 mmol) and dimethyl (1-diazo-2-oxopropyl)phosphonate (0.11 mL, 0.7 mmol), and the mixture was stirred at room temperature for 24 h. The solvent was evaporated, and the residue was partitioned between AcOEt and $H_2O$, and the organic layer was further washed with $H_2O$, followed by brine. The organic layer was dried ($Na_2SO_4$), and evaporated to give the crude **12** (300 mg). To a solution of crude **12** in THF (5 mL) was added a solution of TBAF (1.0 M in THF, 1.2 mL, 1.2 mmol), and the whole was stirred at room temperature for 4 h. The solvent was evaporated, and the residue was suspended MeOH/AcOEt (1:5). The resulting precipitate was collected by filtration to give **13** (148 mg, 2 steps 88%, as a yellow solid). ESI-LRMS *m*/*z* 380 ($MNa^+$); ESI-HRMS calcd for $C_{19}H_{23}N_3O_4Na$ 380.1586, found 380.1500. $^1H$ NMR (DMSO-$d_6$): δ 11.7 (brs, 1 H), 7.73 and 7.49 (each s, each 1 H), 6.63 (brs, 2 H), 5.00 (m, 2 H), 4.80 (t, 1 H, *J* = 6.0 Hz), 4.14 (m, 1 H), 3.76 (m, 1 H), 3.47 (m, 2 H), 2.74 (t, 1 H, *J* = 1.0 Hz), 2.47 (m, 2 H), 2.20 (m, 3 H), 1.68−1.48 (m, 5 H). $^{13}C$ NMR (DMSO-$d_6$): δ 162.46, 158.42, 147.83, 135.34, 133.74, 127.72, 116.66, 105.33, 87.17, 84.49, 74.94, 72.44, 71.20, 62.52, 57.52, 27.57, 23.05, 19.19, 17.56.

**7-(*N*,*N*-Dibutylaminomethylidene)-amino-6-hex-5-ynyl-3-(2-deoxy-β-D-ribofuranosyl)-1*H*-1,8-naphthyridin-2-one (14).** To a suspension of **13** (145 mg, 0.4 mmol) in DMF (4 mL) was added *N*,*N*-dibutylformamide dimethylacetal (0.28 mL, 0.8 mmol), and the mixture was stirred at room temperature for 6 h. The solvent was evaporated, and the residue was purified by a silica gel column, eluted with 3−5% MeOH in $CHCl_3$, to give **14** (87 mg, 44%, as a yellow solid). ESI-LRMS *m*/*z* 497 ($MH^+$); ESI-HRMS calcd for $C_{28}H_{40}N_4O_4Na$ 519.2947, found 519.2958. $^1H$ NMR ($CDCl_3$): δ 9.50 (brs, 1 H), 8.61 (s, 1 H), 7.64 and 7.47 (each s, each 1 H), 5.20 (m, 1 H), 4.66 (brs, 1 H), 4.56 (m, 1 H), 4.12 (m, 1 H), 3.86 (m, 1 H), 3.76 (m, 1 H), 3.49 (m, 2 H), 3.32 (m, 2 H), 3.14 (m, 1 H), 2.93 (brs, 1 H), 2.70 (m, 2 H), 2.48 (m, 1 H), 2.20 (m, 3 H), 1.92 (t, 1 H, *J* = 1.0 Hz), 1.86 (m, 1 H), 1.74−1.51 (m, 7H), 1.41−1.31 (m, 4 H), 0.96−0.86 (m, 6 H); $^{13}C$ NMR ($CDCl_3$): δ 162.21, 155.11, 147.47, 137.59, 135.74, 129.15, 127.78, 113.20, 88.56, 85.96, 80.30, 79.24, 76.90, 68.25, 64.58, 45.83, 41.04, 31.44, 30.81, 29.39, 29.16, 27.97, 20.55, 19.33, 19.02, 13.63, 13.54, 0.11.

**7-(*N*,*N*-Dibutylaminomethylidene)amino-6-hex-5-ynyl-3-(2-deoxy-5-*O*-(4,4′-dimethoxytrityl)-β-D-ribofuranosyl)-1*H*-1,8-naphthyridin-2-one (15).** To a solution of **14** (85 mg, 0.17 mmol) in pyridine (1.7 mL) was added DMTrCl (74 mg, 0.22 mmol), and the whole was stirred at room temperature for 3 h. The reaction was quenched by addition of ice. The mixture was partitioned between AcOEt and $H_2O$, and the organic layer was further washed with $H_2O$, saturated aqueous $NaHCO_3$, and brine. The organic layer was dried ($Na_2SO_4$), and evaporated. The residue was purified by a silica gel column, eluted with 0−2% MeOH in $CHCl_3$, to give **15** (100 mg, 74%, as a yellow foam): ESI-LRMS *m*/*z* 799($MH^+$); ESI-HRMS calcd for $C_{49}H_{58}N_4O_6Na$ 821.4254, found 821.4307. $^1H$ NMR ($CDCl_3$): δ 8.77 (brs, 1 H), 8.50 (s, 1 H), 7.83 (s, 1 H), 7.48 (m, 2 H), 7.37 (m, 4 H), 7.28 (m, 3 H), 7.20 (m, 1 H), 6.81 (m, 4 H) 5.31 (m, 1 H), 4.37 (m, 1 H), 4.08 (m, 1 H), 3.78 (s, 6 H), 3.52 (m, 2 H), 3.36 (m, 4 H), 2.68 (m, 1 H), 2.57 (m, 1 H), 2.20 (m, 2 H), 1.96 (m, 1 H), 1.90 (t, 1 H, *J* = 1.0 Hz), 1.70−1.53 (m, 7H), 1.42−1.33 (m, 4 H), 0.96−0.86 (m, 6 H)). $^{13}C$ NMR ($CDCl_3$): δ 162.34, 158.79, 155.48, 147.49, 146.89, 139.63, 137.80, 136.04, 130.27, 129.28, 127.99, 127.92, 127.75, 127.22, 113.32, 109.72, 88.65, 84.68, 81.58, 79.97, 75.18, 68.37, 63.90, 55.40, 55.35, 52.20, 45.97, 40.98, 31.42, 30.88, 29.42, 29.13, 28.48, 20.52, 19.97, 18.51, 14.05, 13.89, 0.14.

**7-(*N*,*N*-Dibutylaminomethylidene)amino-6-hex-5-ynyl-3-(2-deoxy-5-*O*-(4,4′-dimethoxytrityl)-3-succinate-β-D-ribofuranosyl)-1*H*-1,8-naphthyridin-2-one (16).** To a solution of **15** (93 mg, 0.12 mmol) in MeCN (1.5 mL) were added DMAP (14 mg, 0.12 mmol), $Et_3N$ (0.034 mL, 0.24 mmol), and succinic anhydride (23 mg, 0.24 mmol), and the whole was stirred at room temperature for 12 h. The reaction was quenched by addition of saturated aqueous $NaHCO_3$. The solvent was evaporated and the residue was partitioned between $CHCl_3$ and saturated aqueous $NaHCO_3$, and the extract was washed with brine. The organic layer was dried ($Na_2SO_4$) and evaporated. The residue was purified by a silica gel column, eluted with 1−5% MeOH in $CHCl_3$, to give **16** (73

mg, 70%, as a yellow foam). ESI-LRMS $m/z$ 899 ($MH^+$); ESI-HRMS calcd for $C_{53}H_{62}N_4O_9Na$ 921.4414, found 921.4387. $^1H$ NMR ($CDCl_3$): $\delta$ 10.22 (brs, 1 H), 8.55 (s, 1 H), 7.82 (s, 1 H), 7.45 (m, 2 H), 7.34 (m, 4 H), 7.28 (m, 3 H), 7.20 (m, 1 H), 6.81 (m, 4 H), 5.37 (m, 1 H), 5.22 (m, 1 H), 4.22 (m, 1 H, H-4′), 3.77 (s, 6 H), 3.51 (m, 2 H), 3.36 (m, 4 H), 2.68 (m, 7 H), 2.20 (m, 2 H), 1.96 (m, 1 H), 1.90 (t, 1 H, $J$ = 1.0 Hz), 1.71−1.53 (m, 7H), 1.40−1.33 (m, 4 H), 0.96−0.86 (m, 6 H)). $^{13}C$ NMR ($CDCl_3$): $\delta$ 172.07, 158.60, 156.16, 155.70, 145.04, 139.78, 136.14, 130.30, 130.22, 128.39, 127.95, 126.89, 113.27, 109.17, 84.70, 86.27, 82.89, 76.46, 76.19, 75.52, 68.35, 64.39, 64.36, 55.55, 55.33, 52.06, 45.85, 33.43, 31.46, 31.13, 29.44, 29.20, 28.51, 20.55, 19.97, 18.46, 14.06, 13.92, 0.14.

**7-(*N,N*-Dibutylaminomethylidene)amino-6-hex-5-ynyl-3-(2-deoxy-5-*O*-(4,4′-dimethoxytrityl)-3-succinate-β-D-ribofuranosyl)-1*H*-1,8-naphthyridin-2-one Loaded CPG (Controlled Pore Glass) Support via Succinyl Linker (17).** To a solution of **16** (67 mg, 0.075 mmol) in MeCN (3.0 mL) were added DIEA (90 μL, 0.52 mmol), HOBt (12 mg, 0.09 mmol), HBTU (30 mg, 0.075 mmol), and LCA-CPG (108 μmol/g, 150 mg, 0.015 mmol), and the mixture was kept for 24 h at room temperature. The solid support was filtered and washed with pyridine. The remaining amino groups were capped by treatment with $Ac_2O$ (1.0 mL) and DMAP (48 mg) in pyridine (4.0 mL). The resulting solid support was filtered and washed with MeOH and acetone, and dried under reduced pressure to give **17**. The loading amount was estimated by DMTr cation assay to be 78 μmol/g.

**4-(2-Acetoxyethyl)styrene (19).** To a solution of **18** (2.4 g, 11 mmol) in DMF (20 mL) was added sodium acetate (1.8 g, 22 mmol), and the mixture was heated at 100 °C for 10 h. The mixture was partitioned between AcOEt and $H_2O$, and the organic layer was further washed with $H_2O$ and brine. The organic layer was dried ($Na_2SO_4$), and evaporated. The residue was purified by a silica gel column, eluted with hexane/AcOEt (20:1−10:1), to give **19** (1.34 g, 64%, as a clear oil): ESI-LRMS $m/z$ 191 ($MH^+$); ESI-HRMS calcd for $C_{12}H_{15}O_2$ 191.1072, found 191.1149. $^1H$ NMR ($CDCl_3$): $\delta$ 7.35 (d, 2 H, $J$ = 8.0 Hz), 7.19 (d, 2 H, $J$ = 8.0 Hz), 6.70 (dd, 1 H, $J$ = 11.0 and 17.6 Hz), 5.72 (dd, 1 H, $J$ = 1.0 and 17.6 Hz), 5.22 (dd, 1 H, $J$ = 1.0 and 11.0 Hz), 4.28 (t, 2 H, $J$ = 7.0 Hz), 2.92 (t, 2 H, $J$ = 7.0 Hz), 2.03 (s, 3 H). $^{13}C$ NMR ($CDCl_3$): $\delta$ 171.15, 137.62, 136.65, 136.15, 129.19, 126.49, 113.61, 64.95, 34.95, 21.10.

**4-{(*E*)-2-[4-(2-Acetoxyethyl)phenyl]vinyl}benzoic acid (20).** To a solution of **19** (570 mg, 3.0 mmol) in DMF (3.0 mL) and $Et_3N$ (3.0 mL) were added 4-iodobenzoic acid (1.11 g, 4.5 mmol), $Pd(OAc)_2$ (20 mg, 0.09 mol), and $PPh_3$ (31 mg, 0.12 mmol), and the mixture was heated at 80 °C for 12 h. The solvent was evaporated, and the residue was partitioned between $CHCl_3$ and 1 N HCl aq, and the extract was further washed with $H_2O$, and brine. The organic layer was dried ($Na_2SO_4$) and evaporated. The residue was purified by a silica gel column, eluted with 0−4% MeOH in $CHCl_3$, to give **20** (775 mg, 83%, as a orange solid): mp 218 °C (crystallized from hexane and AcOEt). ESI-MS (LR): $m/z$ 333($MNa^+$); ESI-HRMS calcd for $C_{19}H_{18}O_4Na$ 333.1103, found 333.1136. $^1H$ NMR (DMSO-$d_6$): $\delta$ 12.8 (brs, 1 H), 7.93 (d, 2 H, $J$ = 8.3 Hz), 7.70 (d, 2 H, $J$ = 8.4 Hz), 7.57 (d, 2 H, $J$ = 8.2 Hz), 7.38 and 7.30 (each d, each 1 H, $J$ = 16.4 Hz), 7.28 (d, 2 H, $J$ = 8.0 Hz), 4.22 (t, 2 H, $J$ = 6.8 Hz), 2.90 (t, 2 H, $J$ = 6.8 Hz), 1.98 (s, 3 H). $^{13}C$ NMR(DMSO-$d_6$): $\delta$ 170.25, 167.02, 141.49, 138.17, 134.83, 130.74, 129.73, 129.32, 129.23, 126.87, 126.84, 126.35, 64.14, 20.67/ Anal. Calcd for $C_{19}H_{18}O_4$: C, 73.53; H, 5.85; Found: C, 73.28; H, 5.96.

**1-*O*-*tert*-Butyldimethylsilyl-2-[4-{(*E*)-2-[4-(2-acetoxy)-ethyl]phenyl}vinyl]benzocarbonyl]aminoethanol (21).** To a solution of **20** (155 mg, 0.5 mmol) in DMF (1.0 mL) were added DIEA (170 μL, 1.0 mmol), HOBt (40 mg, 0.3 mmol), and HBTU (227 mg, 0.6 mmol), and the whole was stirred at room temperature. After being stirred for 30 min, *O*-TBS-2-aminoethanol (121 μL, 0.6 mmol) was added to the reaction mixture, and the whole was stirred for another 1.5 h at the same temperature. The reaction was quenched by addition of ice. The mixture was partitioned between AcOEt and $H_2O$, and the organic layer was further washed with $H_2O$, saturated aqueous $NaHCO_3$, and brine. The organic layer was dried ($Na_2SO_4$), and evaporated. The residue was purified by a silica gel column, eluted with hexane/AcOEt (6:1−2:1), to give **21** (170 mg, 73%, as a pale yellow solid); ESI-MS (LR): $m/z$ 468 ($MH^+$); ESI-HRMS calcd for $C_{27}H_{37}NO_4NaSi$ 490.2390, found 490.2346. $^1H$ NMR ($CDCl_3$): $\delta$ 7.75 (d, 2 H, $J$ = 8.3 Hz), 7.56 (d, 2 H, $J$ = 8.3 Hz), 7.46 (d, 2 H, $J$ = 8.1 Hz), 7.22 (d, 2 H, $J$ = 8.0 Hz), 7.17 (d, 1 H, $J$ = 16.3 Hz), 7.08 (d, 1 H, $J$ = 16.3 Hz), 6.54 (t, 1 H, $J$ = 5.4 Hz), 4.29 (t, 2 H, $J$ = 7.0 Hz), 3.80 (t, 2 H, $J$ = 5.3 Hz), 3.59 (t, 2 H, $J$ = 5.3 Hz), 2.95 (t, 2 H, $J$ = 7.0 Hz), 2.05 (s, 3 H), 0.92 (s, 9 H), 0.08 (s, 6 H). $^{13}C$ NMR ($CDCl_3$): $\delta$ 171.13, 167.07, 140.59, 138.04, 135.41, 133.42, 130.43, 129.44, 127.37, 126.98, 126.63, 64.85, 61.99, 42.21, 34.98, 26.04, 21.08, 18.41, −5.18.

**2-[4-{(*E*)-2-[4-(2-Bromo)ethyl]phenyl}vinyl]-benzocarbonyl]aminoethanol (22).** To a solution of **21** (2.6 g, 0.43 mmol) in MeOH (100 mL) was added 28% NaOMe/MeOH (5.6 mL, 28 mmol) at 0 °C dropwise, and the whole was stirred at 0 °C for 40 min. The reaction mixture was neutralized with 1 N HCl aq, and the solvent was evaporated. Then, the residue was partitioned between AcOEt and $H_2O$, and the organic layer was further washed with $H_2O$ and brine. The organic layer was dried ($Na_2SO_4$), and evaporated. To a solution of the residue in $CH_2Cl_2$ (50 mL) were added MsCl (565 μL, 7.3 mmol) and $Et_3N$ (1.0 mL, 7.3 mmol), and the whole was stirred at room temperature for 30 min. The reaction was quenched by addition of ice. The mixture was partitioned between $CHCl_3$ and $H_2O$, and the extract was further washed with saturated aqueous $NaHCO_3$ and brine. The organic layer was dried ($Na_2SO_4$), and evaporated. To a solution of the residue in acetone (28 mL) was added LiBr (1.45 g, 16.8 mmol), and the whole was heated at 65 °C for 1.5 h followed by adding $H_2O$ (20 mL). Then, the mixture was stirred at 85 °C for 2 h. After the solvent was evaporated, the residue was partitioned between AcOEt and $H_2O$, and the organic layer was further washed with $H_2O$ and brine. The organic layer was dried with $Na_2SO_4$, and evaporated. The residue was purified by a silica gel column, eluted with 0−9% MeOH in $CHCl_3$, to give **22** (1.88 g, 3 steps 89%, as a white solid). ESI-LRMS: $m/z$ 374 ($MH^+$); ESI-HRMS calcd for $C_{19}H_{20}BrNO_2Na$ 396.0575, found 396.0486. $^1H$ NMR ($CDCl_3$): $\delta$ 8.40 (t, 1 H, $J$ = 5.5 Hz), 7.86 (d, 2 H, $J$ = 8.4 Hz), 7.66 (d, 2 H, $J$ = 8.3 Hz), 7.57 (d, 2 H, $J$ = 8.2 Hz), 7.30 (d, 2 H, $J$ = 8.0 Hz), 7.36 (d, 1 H, $J$ = 16.3 Hz), 7.27 (d, 1 H, $J$ = 16.3 Hz), 4.71 (t, 1 H, $J$ = 5.0 Hz), 3.74 (t, 2 H, $J$ = 7.1 Hz), 3.51 (m, 2 H), 3.43 (m, 2 H), 3.14 (t, 2 H, $J$ = 7.1 Hz). $^{13}C$ NMR (DMSO-$d_6$): $\delta$ 165.86, 139.73, 138.85, 135.24, 133.18, 129.85, 129.15, 127.62, 127.16, 126.68, 126.11, 59.77, 42.15, 38.10, 34.33.

**1-*O*-{2-Cyanoethyl(diisopropylamino)-phosphinoyloxy}-2-[4-{(*E*)-2-[4-(2-bromo)ethyl]phenyl}-**


dx.doi.org/10.1021/bc500225r | Bioconjugate Chem. 2014, 25, 1360−1369

**vinyl]benzocarbonyl]aminoethanol (23).** To a suspension of **22** (187 mg, 0.5 mmol) in MeCN (5.0 mL) were added DIEA (340 μL, 2.0 mmol) and *N*,*N*-diisopropylchlorophosphramidite (222 μL, 1.0 mmol) at 0 °C, and the whole was stirred at room temperature for 15 min. The mixture was partitioned between $CHCl_3$ and saturated aqueous $NaHCO_3$, and the extract was washed with brine. The organic layer was dried ($Na_2SO_4$) and evaporated. The residue was purified by a silica gel column, eluted with hexane/acetone (4:1−3:1 with $Et_3N$ 1%) to give **23** (182 mg, 62%, as a white syrup): ESI-LRMS *m*/*z* 596 ($MNa^+$); ESI-HRMS calcd for $C_{28}H_{37}BrN_3O_3NaP$ 596.1654, found 596.1603. $^{31}P$ NMR ($CDCl_3$): δ 148.5.

**Preparation of Precursor Oligodeoxynucleotides.** ODNs containing stilbene linker at the 5′-terminus were synthesized on a DNA synthesizer (H-6 DNA/RNA synthesizer) by using $ImO^N$ phosphoramidite, stilbene phosphoramidite, and commercially available deoxyribonucleoside phosphoramidites at 0.2 μmol scale following the standard phosphoroamidite chemistry. The $ImO^N$ and stilbene phosphoramidite were dissolved in dry acetonitrile (0.1 M) and $CH_2Cl_2$ (0.1 M), respectively. The coupling reactions for these phophoroamidites were carried out for 10 min. CPG supporting ODNs was treated with saturated $NaN_3$ in DMF (2 mL) at room temperature for 12 h. The CPG was filtered, washed successively with ethanol and acetone, and dried. ODNs were released from CPG by treatment with 28% aqueous ammonia at 55 °C for 16 h, and the resulting solution was concentrated and purified by reverse-phase HPLC using a linear gradient of 11−22% MeCN in 0.1 M triethylamine-acetate (TEAA) buffer (pH 7.0).

**CuAAC Reaction of ODNs.** A solution of a duplex composed of complementary ODNs (final concentration was 10 μM) was heated in 100 mM MOPS/NaOH buffer (pH 7.0) containing 1 M NaCl at 90 °C for 1 min and allowed to cool to room temperature for 4 h. To a solution of the duplex, $CuSO_4$-tris(benzyltriazolyl)amine (TBTA) in 50% aqueous *t*-BuOH (final concentration: 100 μM) and sodium ascorbate in water (final concentration: 2 mM) were sequentially added. After incubation at 25 °C for 3 h, the mixture was desalted by ethanol precipitation. The resulting cross-linking ODN was analyzed and purified by reverse-phase HPLC using a linear gradient of 5−50% MeCN in 0.1 M TEAA buffer (pH 7.0).

**Enzymatic Digestion for Analyses of Nucleoside Composition.** A mixture of ODN (**ODN 2**: 2.7 μmol, **decoy 1**: 1.3 μmol), snake venom phosphodiesterase (MP Biochemicals, 0.02 mg/mL), nuclease P1 (Yamasa Co., 0.01 unit/μL), and calf intestine alkaline phosphatase (Takara Bio Inc., 0.001 U/μL) in 0.1 M Tris-HCl (pH 7.7) containing 2 mM $MgCl_2$ in a total volume of 200 μL was incubated at 37 °C for 12 h. After the enzymes were deactivated at 100 °C for 3 min, the mixture was concentrated to dryness. Then, the residue was resuspended in $H_2O$ (100 μL) and analyzed by reverse-phase HPLC with a 5−50% MeCN in 0.1 M TEAA buffer (pH 7.0) linear gradient.

**Competition Assay.** $^{32}P$-Labeled contODN (10 nM), NF-κB p50 homodimers (250 ng, Enzo BML-UW9985-0050 NF-κB p50 Subunit, Human), decoy ODN (various concentrations: 1, 10, 20, 50, 100, 200, 300, 500, 800, 1000 nM) in HEPES buffer (10 mM, pH 7.5) containing DTT (1 mM), NaCl (100 mM), poly dI:dC (SIGMA P4929, 5 ng), IGEPAL-CA630 (0.05%), and glycerol (10%) were incubated in a total volume 10 μL at 25 °C for 25 min. The mixture was loaded on 6% native polyacrylamide gel (39:1, acrylamide:bis(acrylamide)), which was precooled and prerun (10 W, 30 min) at 4 °C. The gel was electrophoresed at 10 W (4 °C) for 15 min, and visualized/quantified by FLA9000 Image Scanner (FUJIFILM).

## ■ ASSOCIATED CONTENT

### Ⓢ Supporting Information

Experimental procedure for the synthesis of the CPG-linked ethynyl-$NaN^O$ nucleoside **8**. One scheme and 2 figures as described in the text. This material is available free of charge via the Internet at http://pubs.acs.org.

## ■ AUTHOR INFORMATION

### Corresponding Author

*Phone and FAX: +81-88-633-7288. E-mail: minakawa@tokushima-u.ac.jp.

### Notes

The authors declare no competing financial interest.

## ■ ACKNOWLEDGMENTS

This work was supported by Grant-in-Aid for Scientific Research (B) (Grant Number; 24390027). We would like to thank Mr. H. Kitaike (Center for Instrumental Analysis, The University of Tokushima) for technical supports of analytical data.

## ■ REFERENCES

(1) Latchman, D. S. (1990) Eukaryotic transcription factors. *Biochem. J. 270*, 281−289.

(2) Lee, T. I., and Young, R. A. (2013) Transcriptional regulation and its misregulation in disease. *Cell 152*, 1237−1251.

(3) Rubio-Somoza, L., and Weigel, D. (2013) Coordination of flower maturation by a regulatory circuit of three microRNAs. *PLoS Genet. 9*, e1003374.

(4) Nathan, T. M., Kotoka, N., Robert, D., Shareef, A., Christina, B., Rashmi, T., Richard, A. G., and Hailiang, H. (2013) ATM-dependent MiR-335 targets CtIP and modulates the DNA damage response. *PLoS Genet. 9*, e1003505.

(5) Mann, M. J., and Dzau, V. J. (2000) Therapeutic applications of transcription factor decoy oligonucleotides. *J. Clin. Invest. 106*, 1071−1075.

(6) Xulong, Z., Jian, Z., Lihua, W., Haiming, W., and Zhigang, T. (2007) Therapeutic effects of STAT3 decoy oligodeoxynucleotide on human lung cancer in xenograft mice. *BMC Cancer 7*, 149.

(7) Tomislav, S., Andreas, H. W., Shijun, W., Eva, K., Nicolas, R., Jens, B., Hermann, J. G., and Markus, H. (2009) STAT-1 decoy oligodeoxynucleotide inhibition of acute rejection in mouse heart transplants. *Basic Res. Cardiol. 104*, 719−729.

(8) Maeshima, Y., Kashihara, N., Yasuda, T., Sugiyama, H., Sekikawa, T., Okamoto, K., Kanao, K., Watanabe, Y., Kanwar, S. Y., and Makino, H. (1998) Inhibition of mesangial cell proliferation by E2F decoy oligodeoxynucleotide in vitro and in vivo. *J. Clin. Invest. 101*, 2589−2597.

(9) Sakaue, G., Shimaoka, M., Fukuoka, T., Hiroi, T., Inoue, T., Hashimoto, N., Sakaguchi, T., Sawa, Y., Morishita, R., Kiyono, H., Noguchi, K., and Mashimo, T. (2001) NF-kappa B decoy suppresses xytokine expression and thermal hyperalgesia in a rat neuropathic pain model. *Neuroreport 12*, 2079−2084.

(10) Clusel, C., Ugarte, E., Enjolras, N., Vasseur, M., and Blumenfeld, M. (1993) Ex vivo regulation of specific gene expression by nanomolar concentration of double-stranded dumbbell oligonucleotides. *Nucleic Acids Res. 25*, 3405−3411.

(11) Kunugiza, Y., Tomita, T., Tomita, N., Morishita, R., and Yoshikawa, H. (2006) Inhibitory effect of ribbon-type NF-kappaB decoy oligodeoxynucleotides on osteoclast induction and activity in vitro and in vivo. *Arthritis Res. Ther. 8*, R103.

(12) Nakane, M., Ichikawa, S., and Matsuda, A. (2008) Triazole-linked dumbbell oligodeoxynucleotides with NF-κB binding ability as potential decoy molecules. *J. Org. Chem. 73*, 1842−1851.
(13) Murakami, A., Yamamoto, Y., Namba, M., Iwase, R., and Yamaoka, T. (2001) Photo-cross-linked oligonucleotide duplex as a decoy-DNA for inhibition of restriction endonuclease activity. *Bioorg. Chem. 29*, 223−233.
(14) Osborne, S. E., Vo1lker, J., Stevens, S. Y., Breslauer, K. J., and Glick, G. D. (1996) Design, synthesis, and analysis of disulfide cross-linked DNA duplexes. *J. Am. Chem. Soc. 118*, 11993−12003.
(15) Rostovtsev, V. V., Green, L. G., Fokin, V. V., and Sharpless, K. B. (2002) A stepwise huisgen cycloaddition process: copper(I)-catalyzed regioselective "ligation" of azides and terminal alkynes. *Angew. Chem., Int. Ed. 41*, 2596−2599.
(16) Worrell, B. T., Malik, J. A., and Fokin, V. V. (2013) Direct evidence of a dinuclear copper intermediate in Cu(I)-catalyzed azide-alkyne cycloadditions. *Science 340*, 457−460.
(17) Hikishima, S., Minakawa, N., Kuramoto, K., Fujisawa, Y., Ogawa, M., and Matsuda, A. (2005) Synthesis of 1,8-naphthyridine C-nucleosides and their base-pairing properties in oligodeoxynucleotides: Thermally stable naphthyridine:imidazopyridopyrimidine base-pairing motifs. *Angew. Chem., Int. Ed. 44*, 596−598.
(18) Hikishima, S., Minakawa, N., Kuramoto, K., Ogata, S., and Matsuda, A. (2006) Synthesis and characterization of oligodeoxynucleotides containing naphthyridine:imidazopyridopyrimidine base pairs at their sticky ends. application as thermally stabilized decoy molecules. *ChemBioChem 7*, 1970−1975.
(19) Dogan, Z., Paulini, R., Rojas Stutz, J. A., Narayanan, S., and Richert, C. (2004) 5′-tethered stilbene derivatives as fidelity- and affinity-enhancing modulators of DNA duplex stability. *J. Am. Chem. Soc. 126*, 4762−4763.
(20) Minakawa, N., Kohima, N., Hikishima, S., Sasaki, T., Kiyosue, A., Atsumi, N., Ueno, Y., and Matsuda, A. (2003) New base pairing motifs. The synthesis and thermal stability of oligodeoxynucleotides containing imidazopyridopyrimidine nucleosides with the ability to form four hydrogen bonds. *J. Am. Chem. Soc. 125*, 9970−9982.
(21) Dietrich, B., and Hans-Georg, K. (1963) Über die darstellung einiger p-substituierter styrolderivate. *Monatsh. Chem. 94*, 1250−1261.
(22) Wada, T., Mochizuki, A., Higashiya, S., Tsuruoka, H., Kawahara, S., Ishikawa, M., and Sekine, M. (2001) Synthesis and properties of 2-azidodeoxyadenosine and its incorporation into oligodeoxynucleotides. *Tetrahedron Lett. 42*, 9215−9219.
(23) Abe, N., Abe, H., and Ito, Y. (2007) Dumbbell-shaped nanocircular RNAs for RNA interference. *J. Am. Chem. Soc. 129*, 15108−15109.